Journal of Geodesy manuscript No.
(will be inserted by the editor)

Collocation versus numerical integration in GOCE data analysis

F. Migliaccio[1], **M. Reguzzoni**[1], **F. Sansò**[1], **C. C. Tscherning**[2]

[1] DIIAR, Sezione Rilevamento, Politecnico di Milano, P.za Leonardo da Vinci 32, 20133 Milano, Italy
e-mail: federica.migliaccio@polimi.it; Tel.: +39 02 2399 6507; Fax: +39 02 2399 6530
[2] Department of Geophysics, University of Copenhagen, Juliane Maries Vej 30, 2100 Copenhagen Oe, Denmark
e-mail: cct@gfy.ku.dk; Tel.: +45 35320582; Fax: +45 35365357

Received: date / Revised version: date

Abstract. The space-wise approach to the analysis of satellite borne data, e.g. from the gradiometric mission GOCE, amounts to analysing such data in a way similar to the solution of a boundary value problem. This can be done indeed in several ways, for instance by applying numerical integration formulae, when the boundary functionals have relatively simple forms like T_{rr} or $T_{\lambda\lambda}$, by a least-squares approach or by collocation. In particular this technique can be applied to dense grids of data, e.g. $1^\circ \times 1^\circ$ grids, thanks to the recent implementation of a procedure called Fast Spherical Collocation.

Anyway the practical implementation of all the space-wise methods has to face several problems, such as polar gaps due to the satellite orbit inclination and aliasing effects of the non modelled degrees. In order to better understand their peculiar characteristics, numerical integration and collocation solutions have been compared by applying them to the same simulated data sets, with or without measurement noise. The results of these numerical simulations are described in the paper.

Key words. Gravity field determination, space-wise approach, error comparison

1 Introduction

The mission GOCE (Gravity field and steady-state Ocean Circulation Explorer) is based on the satellite gradiometry principle: it will be continuously tracked by the GPS system, while the on-board three-axis gradiometer, an instrument which assembles pairs of identical accelerometers, will provide the second order derivatives of the gravity potential. The main purpose of this mission is the determination of the stationary gravity field to high accuracy and spatial resolution, for instance in terms of spherical harmonic coefficients up to above degree 200 (cf. ESA, 1999).

In the preparatory work of data analysis two different but complementary approaches have been proposed: the time-wise and the space-wise approach (cf. Rummel et al., 1993). The former is based on a preliminary Fourier transform of time flow of data, exploiting the prevailing block diagonal structure of the normal system to retrieve the harmonic coefficients. Complementary to it, the space-wise approach consists in converting the problem of gravity model estimation into the solution of a boundary value problem for a "sphere" at satellite altitude; basically it consists of two steps: first a frame-transformation and a grid interpolation of the observations along the orbit to homogenize the data and make the numerical solution of the problem feasible, and then the spherical harmonic analysis to estimate the potential coefficients (see Fig. 1).

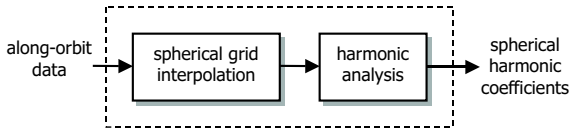

Fig. 1. Basic scheme of the space-wise approach

As for the interpolation, two techniques are available: an elementary local least-squares interpolation, e.g. using polynomial functions, and a collocation solution. The former requires that all the observations to be interpolated carry the same "spatial" information; the latter, instead, may use different functionals adapted to the observation geometry and predict any other functional (for instance the second radial derivatives from the second derivatives along the instrumental z-axis) (cf. Tscherning, 2003). The price to pay for this greater flexibility is the numerical heaviness of collocation in dealing with a large amount of data and with the exact error structure, which is indeed strongly track-wise correlated.

The focus of the paper is on the second step of the space-wise approach, i.e. the harmonic analysis from the boundary data. Again two methods are possible: one is a numerical integration of the data (cf. Migliaccio and Sansò, 1989), exploiting the orthogonality of spherical harmonics; the practical implementation of the method requires a proper discretization of the quadrature formula. The other one is a collocation solution (cf. Tscherning, 2001), which assimilates in a statistical mode a prior knowledge on the field in terms of prior degree variances; it is feasible thanks to a fast numerical algorithm recently implemented, called Fast Spherical Collocation (cf. Sansò and Tscherning, 2003), working with regularly gridded data on parallels, even at different altitudes.

The paper deals with the comparison between these two methods, by applying them to the same simulated data sets, with or without measurement noise. Polar gaps and aliasing effect have been also considered. Working in a typical GOCE framework, all the numerical experiments are based on second radial derivatives, which are the most informative components as well as the easiest to be numerically simulated.

In the following sections we will briefly review the concepts of the two harmonic analysis techniques.

2 Numerical integration

The anomalous potential of the Earth at an arbitrary orbital point with spherical coordinates r, $\sigma \equiv (\theta, \lambda)$ can be written as

$$T(r,\theta,\lambda) = \frac{GM}{R}\sum_{\ell=0}^{\infty}\sum_{m=-\ell}^{\ell}\left(\frac{R}{r}\right)^{\ell+1} T_{\ell m} Y_{\ell m}(\theta,\lambda) \qquad (1)$$

where $Y_{\ell m}$ are the spherical harmonic functions of degree ℓ and order m, and $T_{\ell m}$ are the coefficients of the series expansion (cf. Heiskanen and Moritz, 1967). If we knew the potential T on a boundary sphere S at satellite altitude h, by exploiting the L^2 orthogonality of the base functions

$$\frac{1}{4\pi}\int_S Y_{\ell m}(\theta,\lambda) Y_{kh}(\theta,\lambda) d\sigma = \delta_{\ell k}\delta_{mh} \ , \qquad (2)$$

the harmonic coefficients could be exactly determined by

$$T_{\ell m} = \frac{1}{4\pi\ a_{\ell m}}\int_S T(\theta,\lambda) Y_{\ell m}(\theta,\lambda) d\sigma \qquad (3)$$

where

$$a_{\ell m} = \frac{GM}{R}\left(\frac{R}{R+h}\right)^{\ell+1} \ . \qquad (4)$$

Similar relations can be derived for functionals of T with relatively simple forms, like T_{rr} or $T_{\lambda\lambda}$, only changing the analytical expression of $a_{\ell m}$.

As a matter of fact, we have only some discrete observations of the Earth potential T (or some functionals of T). As a consequence we have to introduce a sort of discretization of the quadrature formula (3) in order to estimate the harmonic coefficients from gridded data. Different solutions are possible (cf. Colombo, 1981): the easiest one can be obviously written as:

$$\hat{T}_{\ell m} = \frac{1}{4\pi\ a_{\ell m}}\sum_{ij} T(\theta_i,\lambda_j) Y_{\ell m}(\theta_i,\lambda_j)|S_{ij}| \qquad (5)$$

where $|S_{ij}|$ is the surface measure of the equiangular block S_{ij}, in which the "reference" sphere S is subdivided. A more refined discretization can be derived under the only approximation that the observed quantity is constant over each block S_{jk} , i.e.

$$\hat{T}_{\ell m} = \frac{1}{4\pi\ a_{\ell m}}\sum_{ij} T(\theta_i,\lambda_j)\int_{S_{ij}} Y_{\ell m}(\theta,\lambda) d\sigma \ . \qquad (6)$$

This method requires recursive computation of the integrals of the associated Legendre functions $P_{\ell m}(\theta)$ over each colatitude interval (cf. Paul, 1978).

Note that the optimal solution, i.e. the solution that minimizes the estimation error of the harmonic coefficients, is often a combination of the two discretized formulae, depending on the grid step and on the functional of T which is observed.

Moreover the numerical integration approach is faced with the problem of polar gaps, due to the orbit inclination, which leaves two unsurveyed areas over the north and south poles. Obviously this lack of data degrades the capability of recovering the harmonic coefficients by formula (5) or (6).

To solve this problem, an iterative solution (see Fig. 2) can be applied; the convergence of the algorithm is theoretically proved under the hypothesis of a finite dimensional gravity model (cf. Albertella et al., 2001) and numerically confirmed when using the discretized formula (6) (cf. Migliaccio and Reguzzoni, 2003). Note that, instead of iteratively repeating the data synthesis on polar gaps and the harmonic analysis on the sphere, it is possible to derive the same solution by applying a linear operator to the gridded data in a direct way, making the computation much faster (see Appendix A).

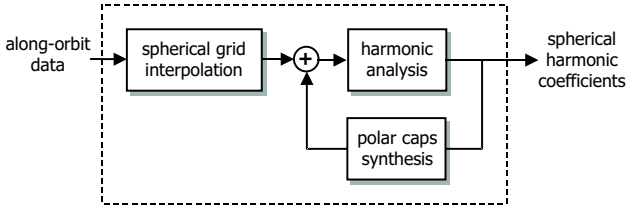

Fig. 2. Scheme of the numerical integration algorithm in the presence of polar gaps

3 Fast Spherical Collocation

First of all, let us consider T as a rotation invariant harmonic random field, i.e.

$$\begin{aligned} &E\left[T_{\ell m}\right] = 0 \\ &E\left[T_{\ell m} T_{kh}\right] = \delta_{\ell k}\delta_{mh}\sigma_\ell^2 \end{aligned} \qquad (7)$$

where σ_ℓ^2 are the so-called degree variances (cf. Kaula, 1966). Suppose we have observations of the potential T, which can be modelled in vectorial notation as

$$\underline{Y} = \underline{T} + \underline{\nu} \qquad (8)$$

where $\underline{\nu}$ is the observational noise with zero mean and known covariance function $C_{\nu\nu}$. We want to determine the spherical harmonic coefficients of the potential. The least-squares

collocation solution (cf. Tscherning, 2001) consists in modelling these coefficients as a linear combination of the observations

$$T_{\ell m} = \underline{\lambda} \cdot \underline{Y} \qquad (\ell, m \text{ fixed}) \tag{9}$$

and then estimating $\underline{\lambda}$ by minimizing the mean square error (Wiener-Kolmogorov principle).

In other words, denoting by $L(T) = T_{\ell m}$ the linear functional which yields the harmonic coefficient of degree ℓ and order m from the potential T, i.e. the analysis operator (3), we have

$$\underline{\lambda} = C_{L[T]T} \left[C_{TT} + C_{\nu\nu}\right]^{-1} \tag{10}$$

where C_{TT} is the covariance matrix of the potential T and $C_{L[T]T}$ is the cross-covariance between the coefficient $T_{\ell m}$ to be estimated and the potential T.

If the observation is a more general functional of the potential (e.g. the radial derivatives or the longitudinal second derivatives), namely

$$\underline{Y} = M\left[\underline{T}\right] + \underline{\nu}\,, \tag{11}$$

the solution of the collocation problem becomes

$$\underline{\lambda} = C_{L[T]M[T]} \left[C_{M[T]M[T]} + C_{vv}\right]^{-1}. \tag{12}$$

Note that, under the hypothesis of rotation invariance, all the involved covariance matrices are functions of the spherical distance ψ between two points P, Q and can be easily derived from

$$C_{TT} = \left(\frac{GM}{R}\right)^2 \sum_{\ell=0}^{\infty} \left(\frac{R^2}{r_P r_Q}\right)^{\ell+1} \sigma_\ell^2 \, P_\ell(\cos\psi) \tag{13}$$

where P_ℓ are the Legendre polynomials of degree ℓ.

Due to its numerical heaviness, the method is usually applied to local patches of data for regional gravity field estimation. However the computational effort can be dramatically reduced if we force the data to fulfill some conditions of regularity. In particular we consider regular grid data on parallels and an observational noise with linearly independent components and with variances depending only on latitude.

By exploiting these conditions, which are not very restrictive in case of geodetic satellite missions like GOCE, a lot of simplifications can be made in the collocation formula (cf. Colombo, 1979), giving rise to a numerically efficient algorithm for the harmonic coefficient estimation, called Fast Spherical Collocation (cf. Sansò and Tscherning, 2003).

Note that this solution allows us to combine different data types, with the only requirement that data are of the same kind on each parallel. This could be used to reduce the negative effect of the polar gaps in the determination of low order coefficients, since it allows the mixing of satellite data with terrestrial or aerial measurements available in the polar areas.

4 Harmonic analysis: comparison of collocation and numerical integration

In order to study the characteristics of the two harmonic analysis methods, a comparison between them has been performed and evaluated based on the following quantities:

– error degree r.m.s. (root mean square)

$$\Delta\sigma_\ell = \sqrt{\sum_m \left(\hat{T}_{\ell m} - T_{\ell m}\right)^2} \tag{14}$$

– error order r.m.s

$$\Delta\gamma_\ell = \sqrt{\sum_\ell \left(\hat{T}_{\ell m} - T_{\ell m}\right)^2} \tag{15}$$

– coefficient relative error

$$\epsilon_{\ell m} = \left|\hat{T}_{\ell m} - T_{\ell m}\right| \Big/ \frac{\Delta\sigma_\ell}{\sqrt{2\ell+1}} \tag{16}$$

where $\hat{T}_{\ell m}$ and $T_{\ell m}$ are the estimated and reference model coefficients respectively. Attention has to be paid to the fact that error order variances $\Delta\gamma_\ell^2$ are just an index of discrepancy and have not much statistical meaning because the population of "order coefficients" is not so homogeneous since it inherits the natural modulus decrease when degree increases.

In the following sections different test cases are presented, describing the results of the numerical simulations.

4.1 The basic test (polar orbit, no aliasing)

The simulated data are second radial derivatives T_{rr} on a spherical grid at satellite altitude ($250\ km$), with grid size equal to $0.72°$; this grid size allows an almost exactly integer partitioning of the latitude interval covered by observations.

Data have been generated all over the sphere, polar caps included, using the EGM96 model (cf. Lemoine et al., 1998) from degree 25 to degree 240.

The harmonic analysis has been performed, both with collocation and with numerical integration, up to degree 240 too, in order to avoid aliasing effects (the Nyquist limit for a $0.72° \times 0.72°$ grid is degree 250). As a consequence all the synthesized harmonic components are also analysed.

Note that in this "ideal" situation no noise is added to the T_{rr} signal; however, for numerical reasons, collocation requires the use of an error covariance matrix, which has been chosen diagonal, with a standard deviation of $0.5\ mE$ (the minimum acceptable value).

First of all, we have compared the two methods on the basis of the error degree r.m.s. in Fig. 3 and of the error order r.m.s. in Fig. 4. The integration approach shows a much smaller error than collocation in the highest degrees (note the logarithmic scale in Fig. 3). On the other hand, the better behaviour of collocation in the low-medium degrees is mainly due to its capability of better estimating low order coefficients, in particular orders 0 and 1 as shown in Fig. 5.

But how is the error distributed coefficient by coefficient? The relative errors in Fig. 6 and Fig. 7 show a completely different behaviour of the two analysis methods. Collocation errors mainly depend on the coefficient degree: this is due to the a-priori information on the covariance function given in terms of degree variances. The integration error distribution is practically uniform, a part from low order coefficients which are estimated with a worse result. Altogether the error comparison (see Fig. 8) suggests a combined solution, applying collocation for low degrees and for very low orders and the integration approach elsewhere.

4.2 The aliasing effect test

In a real situation, there is always a part of the signal which is not modelled in the analysis procedure, since we can estimate finite dimensional models only.

In order to obtain a more realistic simulation, data have been generated from degree 25 to degree 360, still using the EGM96 model and the previously defined simulation parameters; no noise has been added to T_{rr} data.

Of course this data-set produces aliasing, namely a folding of power from higher frequency components into the lower ones. Let us recall that working with an equiangular spherical grid of step Δ the Nyquist limit, i.e. maximum degree L to which the harmonic analysis can be extended, is given by $L = 180^\circ/\Delta$ (e.g. for $\Delta = 0.72^\circ$, $L = 250$).

If we compare this case with the results of the basic test, the collocation solution shows no significantly changes both in the error degree r.m.s. (Fig. 9) and error order r.m.s. (Fig. 10). The integration approach, instead, presents a negligible error increase at high degrees and a strange alteration at medium orders. However further simulations up to degree 720 with GPM98 model (cf. Wenzel, 1998) show that the error order r.m.s. quickly becomes stable (see Fig. 11), meaning that the aliasing effect is only due to the first non modelled components over degree 240.

Furthermore the collocation error distribution (Fig. 12) does not change thanks to the damping of high degrees corresponding to the prior information on the degree variances. In other words, collocation is robust against aliasing. As for the numerical integration, the effect of the unmodelled harmonic components is more visible (Fig. 13), but it does not significantly modify the comparison between the two analysis methods (Fig. 14).

4.3 The polar gaps test

The GOCE satellite will fly in a sun-synchronous orbit at a low altitude (about $250\ km$). Due to the orbit inclination (about 96.5°), no observations will be collected over the polar caps. Simulated gridded data has been generated accordingly.

In order to study separately the effect of the polar gaps on the harmonic coefficients recovery, no aliasing has been considered, i.e. data have been synthetized and analysed up to degree 240. Again no noise has been added to the T_{rr} data.

The error degree r.m.s. (Fig. 15) increase in both cases, though collocation errors practically do not change at high degrees due to the a priori information on the signal degree variances. The polar gaps effect is clearly seen in the error order r.m.s. (Fig. 16): as expected it affects the first orders only, while higher orders are not involved at all. Now the better behaviour of the collocation method is evident at least up to order 15-20 (Fig. 17).

As for the coefficient error distribution, the polar gaps cause a worse estimation of the lower order coefficients in both the collocation (Fig. 18) and integration approach (Fig. 19). This is a well-known results in geodetic literature (cf. Sneeuw and van Gelderen, 1997). However a comparison of the two methods clearly shows that collocation is more robust than integration against this deterioration. Altogether, if no data are available on polar caps, a combined solution should be based on collocation at low degrees and orders and on numerical integration elsewhere (Fig. 20).

4.4 The noisy data set test

Finally let us consider a still more realistic simulation with noisy data. A gaussian white-noise with an error r.m.s. of $1\ mE$ (realistic after gridding along-orbit data) was added to gridded T_{rr} data.

Aliasing was taken into account too (T_{rr} synthetized up to degree 360). Two cases were considered: with and without polar gaps.

The results, in terms of error degree r.m.s. (see Fig. 21 and Fig. 22), show that collocation and integration are very similar in the presence of noisy data, though collocation tends to be more robust against polar gaps. Anyway the use of a space-wise approach in a realistic simulation seems to allow for the reconstruction of the gravity field up to degree 200 and above with sufficient accuracy.

5 Conclusions

In this paper the Fast Spherical Collocation algorithm and the numerical integration approach have been compared: the former works better at low degrees and orders, the latter at high frequency components. This suggests combined solutions.

When noisy data have been considered, the two methods prove to be almost equivalent, at least in terms of error estimates. However collocation, exploiting the a-priori information on the signal degree variances, seems to be more robust against aliasing and polar gap effects.

From the computational point of view, both methods prove to be numerically efficient, since they can retrieve spherical harmonic coefficients in few minutes using a standard PC.

As a final conclusion we can state that the space-wise approach to GOCE data analysis can rely on two different and independent solutions. They can (and should) be used to cross check the results.

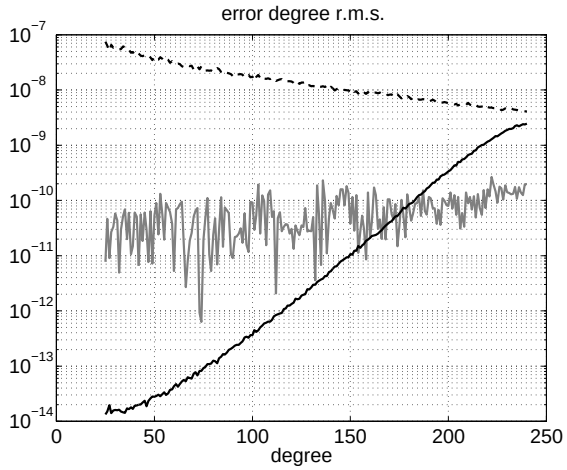

Fig. 3. Collocation (black) and numerical integration (grey) error degree r.m.s. for the basic test. The dotted curve represents the EGM96 model degree variances

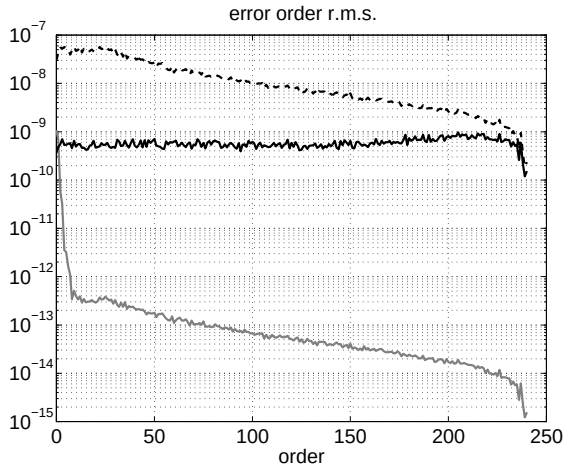

Fig. 4. Collocation (black) and numerical integration (grey) error order r.m.s. for the basic test. The dotted curve represents the EGM96 model order variances

Fig. 5. Collocation (black) and numerical integration (grey) error order r.m.s. for the basic test and lower orders. The dotted curve represents the EGM96 model order variances

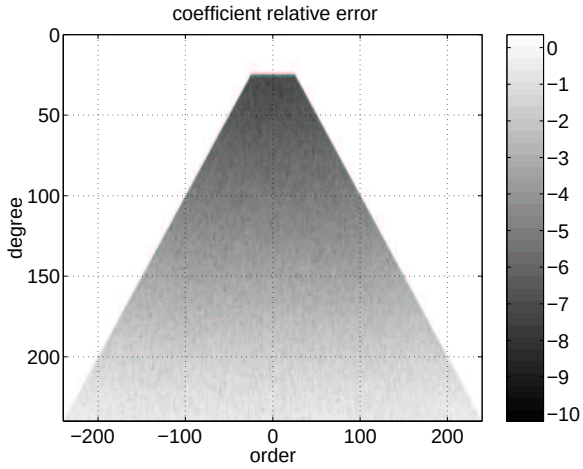

Fig. 6. Collocation error distribution for the basic test

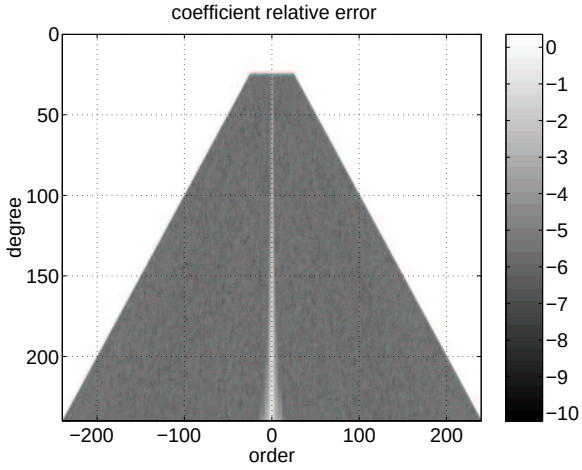

Fig. 7. Numerical integration error distribution for the basic test

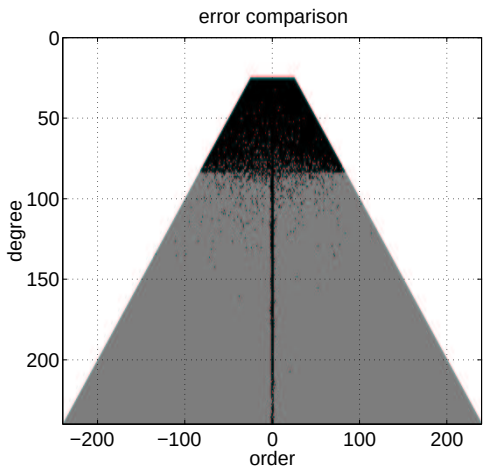

Fig. 8. Error comparison for the basic test: coefficients in black are better estimated by collocation while coefficients in grey by numerical integration

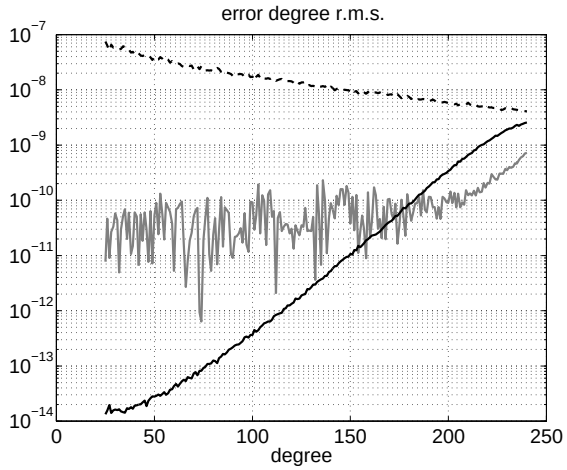

Fig. 9. Collocation (black) and numerical integration (grey) error degree r.m.s. in the presence of aliasing. The dotted curve represents the EGM96 model degree variances

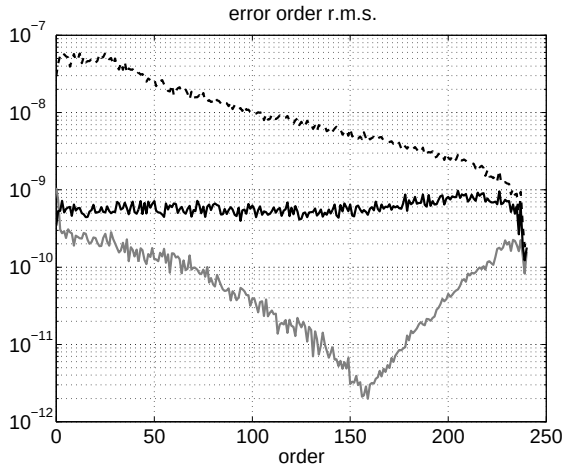

Fig. 10. Collocation (black) and numerical integration (grey) error order r.m.s. in the presence of aliasing. The dotted curve represents the EGM96 model order variances

Fig. 11. Numerical integration error order r.m.s. as a function of the maximum degree L. For values of L close to the Nyquist limit, the aliasing only spreads at low and high orders; increasing the values of L, it quickly becomes stable. The dotted curve represents the error order r.m.s. without aliasing

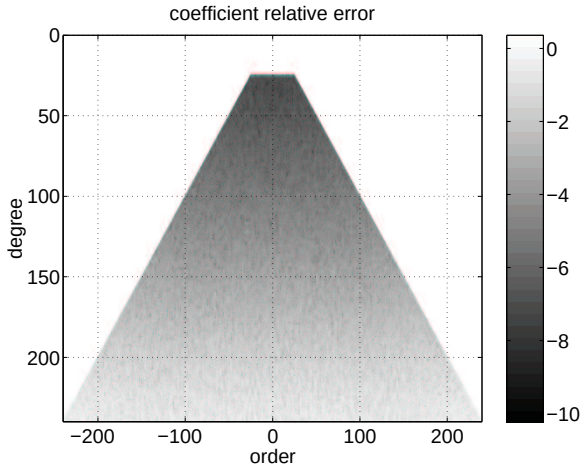

Fig. 12. Collocation error distribution in the presence of aliasing

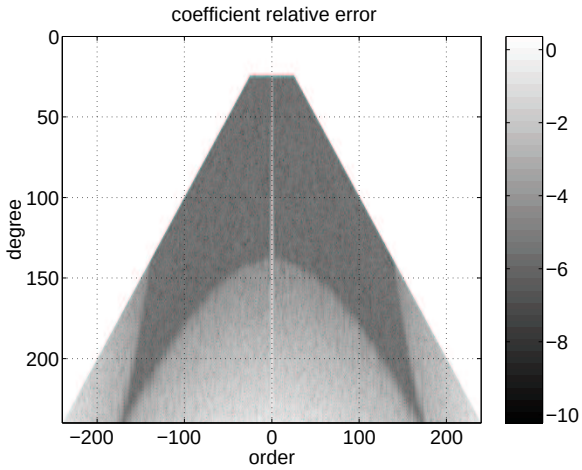

Fig. 13. Numerical integration error distribution in the presence of aliasing

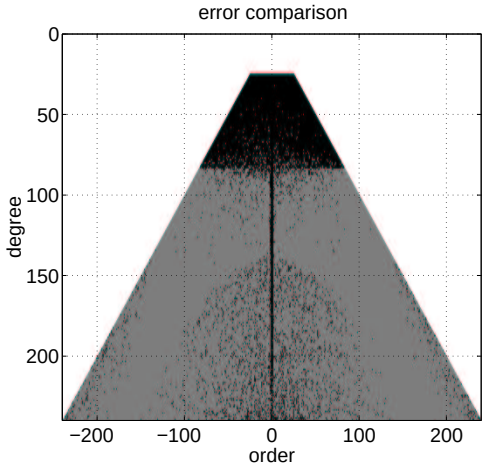

Fig. 14. Error comparison in the presence of aliasing: coefficients in black are better estimated by collocation while coefficients in grey by numerical integration

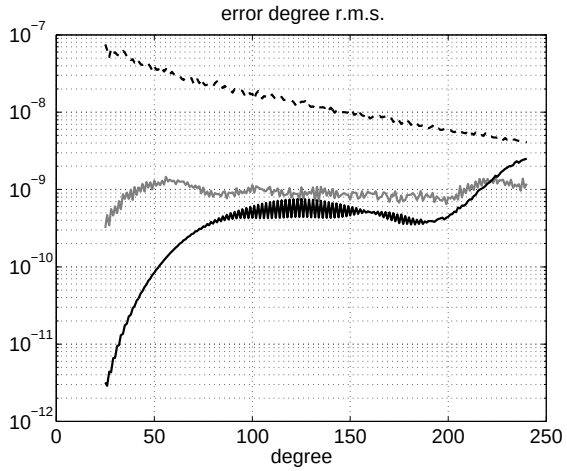

Fig. 15. Collocation (black) and numerical integration (grey) error degree r.m.s. in the presence of polar gaps. The dotted curve represents the EGM96 model degree variances

Fig. 16. Collocation (black) and numerical integration (grey) error order r.m.s. in the presence of polar gaps. The dotted curve represents the EGM96 model order variances

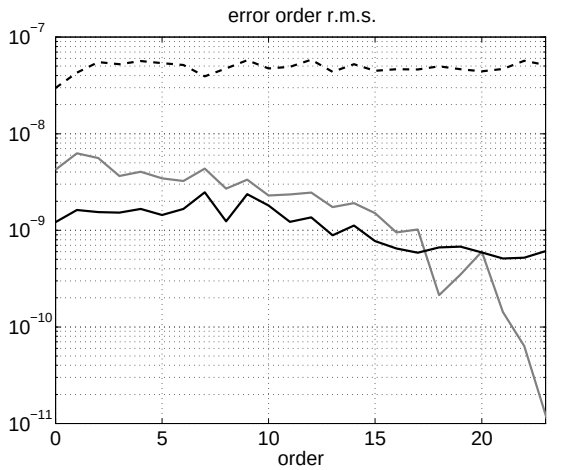

Fig. 17. Collocation (black) and numerical integration (grey) error order r.m.s. in the presence of polar gaps and for lower orders. The dotted curve represents the EGM96 model order variances

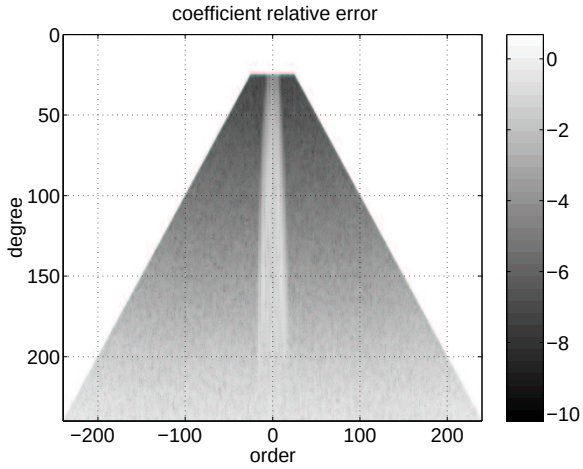

Fig. 18. Collocation error distribution in the presence of polar gaps

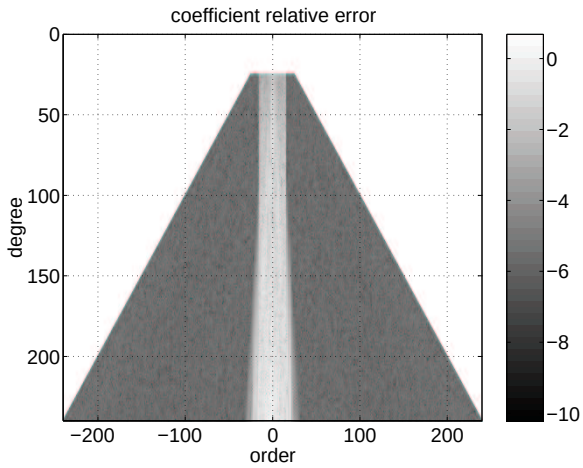

Fig. 19. Numerical integration error distribution in the presence of polar gaps

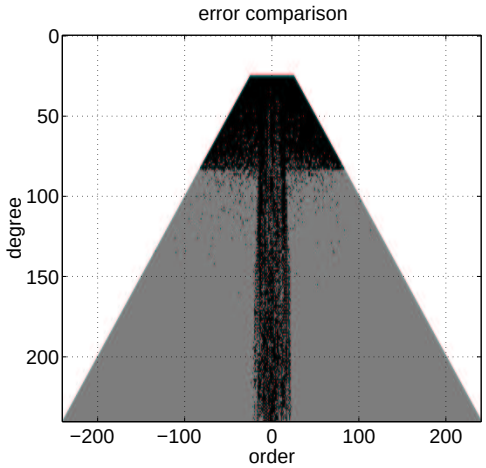

Fig. 20. Error comparison in the presence of polar gaps: coefficients in black are better estimated by collocation while coefficients in grey by numerical integration

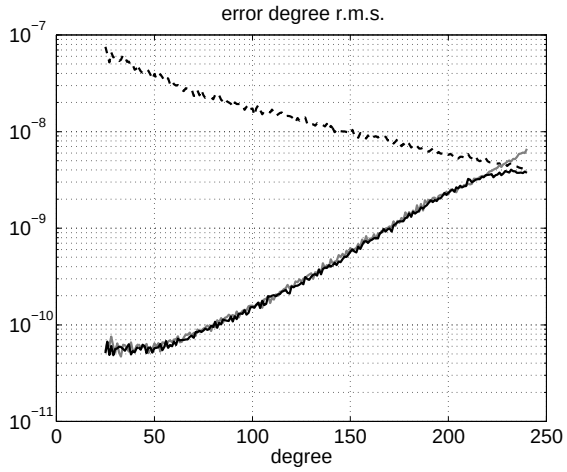

Fig. 21. Collocation (black) and numerical integration (grey) error degree r.m.s. in the presence of noise and aliasing. The dotted curve represents the EGM96 model degree variances

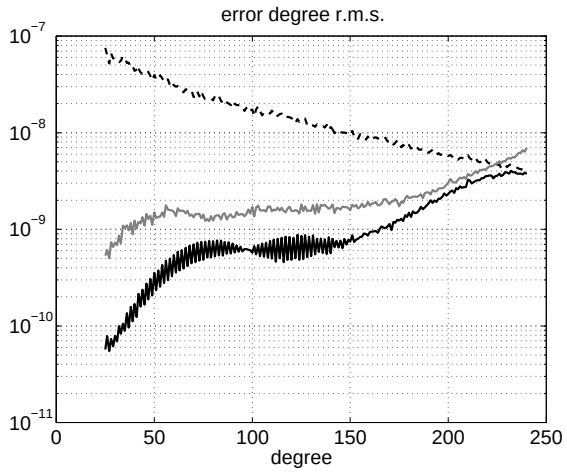

Fig. 22. Collocation (black) and numerical integration (grey) error degree r.m.s. in the presence of noise, aliasing and polar gaps. The dotted curve represents the EGM96 model degree variances

Appendix A

The harmonic analysis operator in the presence of polar gaps

As already seen in the paper, the numerical integration approach consists in estimating the gravity field model by exploiting the orthogonality of spherical harmonic functions all over a reference sphere at satellite altitude. In this appendix we discuss how to define a (linear) integration operator if no data are available on the polar caps. The method can be easily generalized to any type of data gaps.

The starting point is always the equation (3), but now the reference sphere S is partitioned into the polar caps P and the belt B so that $P \cup B = S$ and $P \cap B = \emptyset$; in this way the quadrature formula can be divided into two parts

$$\begin{aligned} T_{\ell m} &= \frac{1}{4\pi\ a_{\ell m}} \int_P T(\theta,\lambda) Y_{\ell m}(\theta,\lambda) d\sigma + \\ &+ \frac{1}{4\pi\ a_{\ell m}} \int_B T(\theta,\lambda) Y_{\ell m}(\theta,\lambda) d\sigma = \\ &= T^P_{\ell m} + T^B_{\ell m}\ . \end{aligned} \tag{A1}$$

Let us concentrate on the first term. Here the use of the more accurate discretization (6) is strictly recommended due to the high variability of the spherical harmonic functions $Y_{\ell m}$ on the polar areas, especially for low orders m, depending on the factor $\sin^m(\theta)$ in the definition of $P_{\ell m}$. In other words, we can write

$$T^P_{\ell m} \cong \frac{1}{4\pi\ a_{\ell m}} \sum_{ij} T(\theta_i,\lambda_j) \int_{P_{ij}} Y_{\ell m}(\theta,\lambda) d\sigma \tag{A2}$$

where P_{ij} are the equiangular $(\Delta \times \Delta)$ blocks, in which the polar caps are subdivided.

Since the Earth potential T or some of its functionals are not observed on the polar areas, introducing the synthesis operator (1) extended to a maximum degree L, we can express the observables $T(\theta_i,\lambda_j)$ as a function of the unknown harmonic coefficients, i.e.

$$\begin{aligned} T^P_{\ell m} &\cong \frac{1}{4\pi\ a_{\ell m}} \sum_{ij} \sum_{k=0}^{L} \sum_{h=-k}^{k} a_{kh} T_{kh} Y_{kh}(\theta_i,\lambda_j) \cdot \\ &\cdot \int_{P_{ij}} Y_{\ell m}(\theta,\lambda) d\sigma = \\ &= \frac{1}{4\pi\ a_{\ell m}} \sum_{ij} \sum_{k=0}^{L} \sum_{h=-k}^{k} a_{kh} T_{kh} P_{kh}(\theta_i) \begin{pmatrix} \cos h\lambda_j \\ \sin h\lambda_j \end{pmatrix} \cdot \\ &\cdot \int_{\theta_i - \frac{\Delta}{2}}^{\theta_i + \frac{\Delta}{2}} P_{\ell m}(\theta) \sin(\theta) d\theta \int_{\lambda_j - \frac{\Delta}{2}}^{\lambda_j + \frac{\Delta}{2}} \begin{pmatrix} \cos m\lambda \\ \sin m\lambda \end{pmatrix} d\lambda\ . \end{aligned} \tag{A3}$$

Solving the integral

$$\int_{\lambda_j - \frac{\Delta}{2}}^{\lambda_j + \frac{\Delta}{2}} \begin{pmatrix} \cos m\lambda \\ \sin m\lambda \end{pmatrix} d\lambda = \Delta\ \mathrm{sinc}\tfrac{m\Delta}{2} \begin{pmatrix} \cos m\lambda_j \\ \sin m\lambda_j \end{pmatrix} \tag{A4}$$

and taking into account the orthogonality of the sinusoidal functions on a regular discrete array, we have

$$\begin{aligned} T^P_{\ell m} &\cong \frac{1+\delta_{m,0}}{4\ a_{\ell m}}\ \mathrm{sinc}\tfrac{m\Delta}{2} \sum_{k=0}^{L} a_{km} T_{km} \cdot \\ &\cdot \sum_i P_{km}(\theta_i) \int_{\theta_i - \frac{\Delta}{2}}^{\theta_i + \frac{\Delta}{2}} P_{\ell m}(\theta) \sin(\theta) d\theta \end{aligned} \tag{A5}$$

where δ is the Kronecker delta and $\mathrm{sinc}(\cdot)$ is the sine cardinal function.

Substituting equation (A5) into the "global" quadrature formula (A1), we get a simply determined equation system, which can be written in vectorial notation as follows

$$\underline{T} = K\underline{T} + H\underline{U} + \underline{\eta} \tag{A6}$$

where

- K is the matrix whose generic element can be easily derived from equation (A5);
- H is the harmonic analysis matrix, computed by using the discretization (5) or (6) or a combination of them;
- $\underline{T}$ is the vector of the unknown coefficients;
- $\underline{U}$ is the vector of observations without noise (Earth potential values or some other functionals);
- $\underline{\eta}$ is the vector of the discretization error.

On the other hand, since we have only an observed (noisy) vector $\underline{U}_0$ and we do not know $\underline{\eta}$, the harmonic coefficients can be estimated as

$$\hat{\underline{T}} = (I - K)^{-1}\, H\, \underline{U}_0 \tag{A7}$$

which corresponds to applying a discretized quadrature formula on the available data, e.g. filling the gaps with zero values, and then correcting the estimated coefficients through $(I - K)^{-1}$ in order to consider the effect of the polar gaps.

Note that the solution (A7) can also be computed iteratively, i.e.

$$\underline{T}^{(n+1)} = K\underline{T}^{(n)} + H\underline{U}_0 \tag{A8}$$

since all the eigenvalues of the matrix K are in modulus less than 1. This corresponds to the iterative scheme in Fig. 2, which is however slowly convergent because many eigenvalues tend to approach 1 when the maximum degree L increases.

Let us conclude with some numerical remarks.

First of all, one could object that the matrix K, and consequently $(I - K)$, is not symmetric, making the inversion procedure more complicated. However, to overcome the problem, one can go back to equation (A5) and observe that the generic element of K is proportional to the term

$$P_{km}(\theta_i) \int_{\theta_i - \frac{\Delta}{2}}^{\theta_i + \frac{\Delta}{2}} P_{\ell m}(\theta) \sin(\theta) d\theta \,, \tag{A9}$$

which was derived as the discretization of the integral

$$\int_{\theta_i - \frac{\Delta}{2}}^{\theta_i + \frac{\Delta}{2}} P_{km}(\theta) P_{\ell m}(\theta) \sin(\theta) d\theta = - \int_{t_2}^{t_1} P_{km}(t) P_{\ell m}(t) dt \,. \tag{A10}$$

Considering that the Legendre function with the lower degree has a smoother behaviour, the discretization (A10) is generally more accurate when $k < \ell$; a reasonable way to make the matrix K symmetric, achieving at the same time a better approximation, is therefore to compute *all* the terms (A9) integrating the Legendre function with the higher variability, i.e. with the higher degree, and fixing the smoother one.

Another numerical improvement can be obtained by properly reordering the unknowns, which are to be grouped by order in the vector $\underline{T}$. In this way the matrices K and $(I - K)$ have the usual block diagonal structure, the largest block being of dimension $(L + 1) \times (L + 1)$. The inversion of such matrices is therefore feasible and fast.

References

Albertella A, Migliaccio F, Sansò F (2001) Data gaps in finite-dimensional boundary value problems for satellite gradiometry. J. Geod. 75: 641-646

Colombo OL (1979) Optimal estimation from data regularly sampled on a sphere with applications in geodesy. Report 291, Dept. of Geodetic Science, The Ohio State University, Columbus, Ohio

Colombo OL (1981) Numerical methods for harmonic analysis on the sphere. Report 310, Dept. of Geodetic Science, The Ohio State University, Columbus, Ohio

ESA (1999) Gravity Field and Steady-State Ocean Circulation Mission. ESA SP-1233 (1). ESA Publication Division, c/o ESTEC, Noordwijk, The Netherlands

Lemoine FG, Kenyon SC, Factor JK, Trimmer RG, Pavlis NK, Chinn DS, Cox CM, Klosko SM, Luthcke SB, Torrence MH, Wang YM, Williamson RG, Pavlis EC, Rapp RH, Olson TR (1998) The development of the joint NASA GSFC and NIMA geopotential model EGM96. NASA/TP-1998-206861, Goddard Space Flight Center, Greenbelt, Maryland

Heiskanen WA, Moritz H (1967) Physical geodesy. WH Freeman, San Francisco

Kaula WM (1966) Theory of satellite geodesy. Blaisdell Publishing Company, Waltham

Migliaccio F, Sansò F (1989) Data Processing for the Aristoteles Mission. Proceedings of the Italian Workshop on the European Solid-Earth Mission Aristoteles, Trevi, 30-31 May 1989, pp 91-123

Migliaccio F, Reguzzoni M (2003) Gravity from space: the state of space-wise approach. Proceedings of the First Workshop on International Gravity Field Research, Graz. In print

Paul MK (1978) Recurrence relations for integrals of associated Legendre functions. Bull Geod 52: 177-190

Rummel R, Van Gelderen M, Koop R, Schrama E, Sansò F, Brovelli MA, Migliaccio F, Sacerdote F (1993) Spherical harmonic analysis of satellite gradiometry. Netherlands Geodetic Commission Publications on Geodesy, New Series, Number 39, Delft, The Netherlands

Sansò F, Tscherning CC (2003) Fast spherical collocation: theory and examples. J. Geod. 77: 101-112

Sneeuw N, van Gelderen M The Polar Gap. In: Geodetic Boundary Value Problems in View of the One Centimeter Geoid, Sansò F and Rummel R eds, Lecture notes in Earth Sciences, 65, Springer, Berlin

Tscherning CC (2001) Computation of sherical harmonic coefficients and their error estimates using least-squares collocation. J. Geod. 75: 12-18

Tscherning CC (2003) Testing gridding and filtering of GOCE gradiometer data by Least-Squares Collocation using sumulated data. Submitted proceedings of the IUGG General Assembly, Sapporo, July 2003

Wenzel HG (1998) Ultra hochauflösende Kugelfunktionsmodelle GPM98A und GPM98B des Erdschwerefeldes. Proceedings Geodatische Woche, Kaiserslautern